Optical microbottle resonator with polyvinyl alcohol coating for sodium alginate concentration sensing

AMINAH AHMAD[1,*], MOHD HAFIZ JALI[2], HAZIEZOL HELMI MOHD YUSOF[3], MD ASHADI MD JOHARI[1], SULAIMAN WADI HARUN[4]

[1]*Faculty of Electrical and Electronic Engineering Technology, Universiti Teknikal Malaysia Melaka, 76100 Melaka, Malaysia*

[2]*Faculty of Electrical Engineering, Universiti Teknikal Malaysia Melaka, 76100 Melaka, Malaysia*

[3]*Faculty of Electronic and Computer Engineering, Universiti Teknikal Malaysia Melaka, 76100 Melaka, Malaysia*

[4]*Department of Electrical Engineering, Faculty of Engineering, University of Malaya, 50603 Kuala Lumpur, Malaysia*

The research paper defined the effect of polyvinyl alcohol (PVA) coating on optical microbottle resonator (MBR) for sodium alginate concentration sensor. The resonator made from silica fiber SMF28 used a technique known as "soften-and-compress". The MBRs size is based on the three parameters, which is bottle diameter (D_b), stem diameter (D_s) and bottle length (L_b). The MBR was then coated with PVA and named MBR-PVA-A, MBR-PVA-B and MBR-PVA-C. The coated MBR-PVA was then coupled with microfiber for characterisation and able to have Q-factor >10^5 for all conditions. The MBR-PVAs were then used for the sodium alginate sensor with liquid concentrations ranging from 1% to 6%. The MBR-PVAs performance is ultimately excellent, where the results are based on transmitted power and wavelength shift analysis. The MBR-PVAs are promising as sodium alginate concentration sensors by the sensitivity, linearity, stability, and repeatability performance.

(Received June 29, 2021; accepted April 7, 2022)

Keywords: Optical Microresonator, Microbottle Resonator, Sodium Alginate

1. Introduction

Fiber optic captured intention widely in communication and non-communication applications [1-5]. Optical microresonator (OMR) is a fiber optic sub-creation explored in various applications [6, 7]. Recently, the OMR operated by whispering gallery modes (WGM) was then applied in laser, sensor and plasmonic devices [8-10]. The modes in the OMRs then narrowed spatially and transiently, increased optical forces, promising quality factor and extending the lifetime of photons. By this concept, the OMRs may be constructed in numerous structures such as microring, microdisc, micropillar and microsphere [11-14]. WGMs on optical resonators then seriously explored different preferences such as tremendous quality factor, decaying in intrinsic losses, and modest assembly methods [15, 16]. This paper promotes one class of the OMR known as microbottle structure resonator (MBR), made from optical silica fiber with a bump in the midriff, which is of fibre, similar to bottle look. The WGMs freely coursed across the MBR surface, opposite the bottle axis, making this resonator valued in sensing application. However, an electromagnetic field on the MBR surface cooperates with the sensing medium as part of sensor application [6, 17-19]. It made the MBR slightly similar due to the concept of potation with surface plasmon-polaritons (SPPs) electromagnetic fields [20, 21]. Hence, the MBR proving exceeds the quality factor and free spectral range (FSR), suitable as a sensor application [22-24]. The MBR previously showed tremendous performance in several sensing applications such as temperature, humidity and gas sensors [25-29].

This article promoted the coating MBR as a sodium alginate sensor. Several experimental research on sodium alginate sensors have been explored but non-other resonator used for it, as Table 1. This sodium alginate, known as salt from the alginic acid used to retain the water in meat, increases elasticity and improves the product's freshness [30, 31]. The coating material used is polyvinyl alcohol, chosen due to the similarity refractive index with the MBR base material, 1.4793 for polyvinyl alcohol and 1.4515 for silica fiber. The coating may increase the MBR size, producing high quality factors and FSR [32, 33]. The MBR-PVA coating is the first type of resonator used as a sodium alginate sensor. The experiment began by forming three different MBR sizes utilising a technique known as "soften-and-compress", then coating with the PVA by the "drop-casting" technique. The coated MBR-PVAs are then excited with microfiber 2μm diameter for characterisation to ensure the resonator is ready to be used as a sensor [34, 35]. The sodium alginate was prepared in liquid form with a range of concentrations from 1% to 6%. The MBR-PVAs is performed as a sodium alginate sensor by determining the sensitivity, linearity, stability and repeatability results. These parameters may obtain the capability of the MBR-PVAs as a sodium alginate concentration sensor.

Table 1. List of reported research on sodium alginate sensor

No.	Title	Publish Date	Sensitivity
1.	Green, in situ fabrication of silver/poly(3-aminophenyl boronic acid)/ sodium alginate nano gel and hydrogen peroxide sensing capacity	2020	0.0022 ΔA/μM
2.	Carbon dots—Sodium alginate hydrogel: A novel tetracycline fluorescent sensor and adsorber	2019	0.109 I/nm

2. Characterisation of MBR-PVAs

The MBR was formed using silica fiber SMF28 by a method known as "soften-and-compress", where the WGM was utilised for spectral characteristic [35]. The bottle structure on the midriff fiber is formed using the splicing machine (Furukawa Electric Fitel S178A) by heating that area with an electrical arc. The fiber is compressed direction inwards from both right and left sides simultaneously. The size of the bottle is determined by the number of arcs applied during the heating process [22]. The MBR structure is shown in Fig. 1, characterised by three parameters of bottle diameter D_b, bottle stem diameter D_s, and bottle length L_b, similar to previous works [22]. The microfiber with a $2\mu m$ diameter used together with the MBR for characterisation and sensing procedure is then fabricated using a method known as "flame brushing" [36, 37]. Three sizes of the MBR used in this experiment showed in Table 2. The MBRs than experienced procedure known as "drop-casting" allowed the PVA to be coated on the top of the MBRs surface, as shown in Fig. 2. The PVA coating solution was prepared by dissolving 5 mg PVA with 12 ml of distilled water and stirred for 6 hours long inside the ultrasonic cleaning machine (GT SONIC-P2). The coating MBRs was left to dry for 24 hours long. The coating thickness was measured to have $10\mu m$ for all MBR, respectively. The coating MBRs than named as MBR-PVA-A, MBR-PVA-B and MBR-PVA-C.

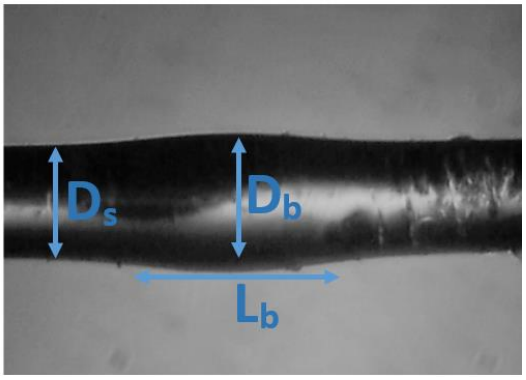

Fig. 1. The MBR with parameter of L_b = 183 μm, D_b = 180 μm and D_s = 125 μm

Table 2. The size of the MBR before the coating procedure

Parameter	Bottle diameter, D_b	Bottle stem diameter, D_s	Bottle length, L_b
MBR-A	170 μm	125 μm	182 μm
MBR-B	180 μm	125 μm	183 μm
MBR-C	190 μm	125 μm	184 μm

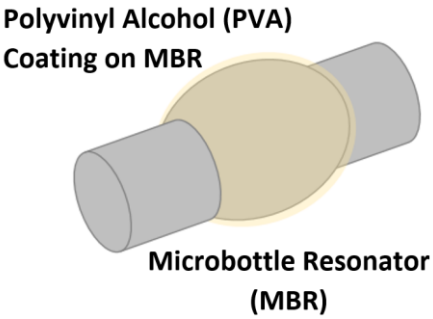

Fig. 2. The MBR experienced the "drop-casting" method for PVA coating

Before being applied for sensing purposes, the MBR-PVAs are then characterised for quality factor and FRS results. The tunable laser source (ANDOAQ4321D) supplied a wavelength for the experiment, ranging from 1551 nm to 1551.3. This tunable laser source was perfectly suitable to be used because of the capability to generate a wavelength range from 1520 nm to 1620 nm with 0.001 nm intervals perfectly. The wavelength used for the MBR characterisation could be in any range, and the best range is 1550 nm. However, 1551 nm is selected to be used in this procedure to widen the potential of the MBR and allow the MBR to work in the different wavelength ranges. The final transmitted power was collected by an optical spectrum analyser (OSA, Anritsu MS9710C). As a result, Fig. 3 showed the transmission spectral with promising quality factor by the size of the MBR-PVA [38]. All coating resonators manage to have different insertion loss values where the MBR-PVA-A is -32dBm, which is higher than others. The insertion loss may differ for each MBR-PVAs due to the coupling distance between the MBR-PVAs with microfiber and the coating thickness on the resonator surface [27, 39]. Free-space radian modes, over-coupled with the microfiber and numbers of partially overlapping may also cause different insertion losses in spectral transmission [38, 40]. Therefore, the depth and the number of the resonant from the transmitted spectral may change due to the size of the MBR-PVAs.

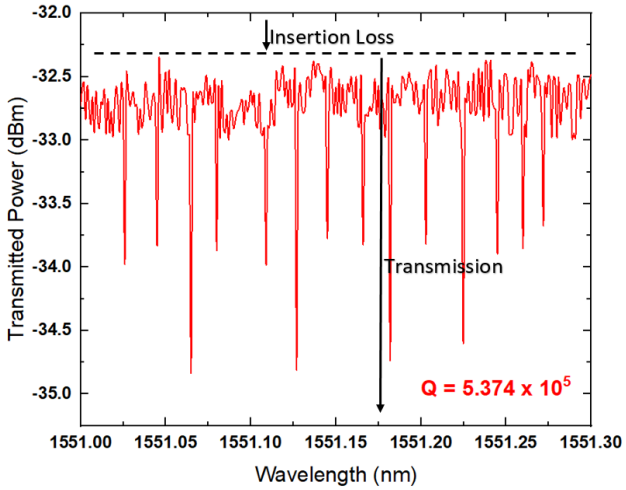

MBR-PVA-A

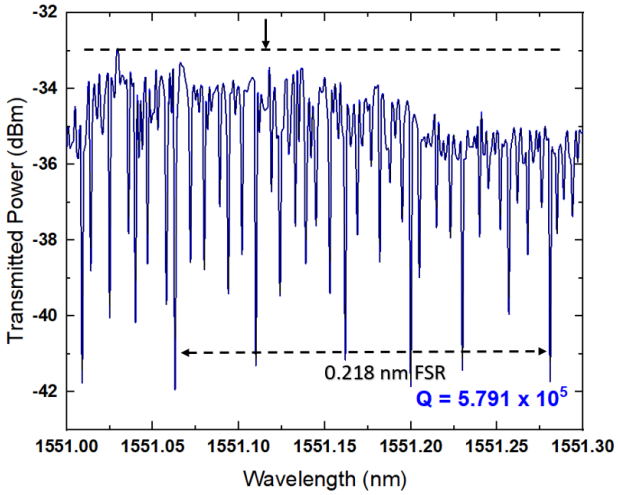

MBR-PVA-B

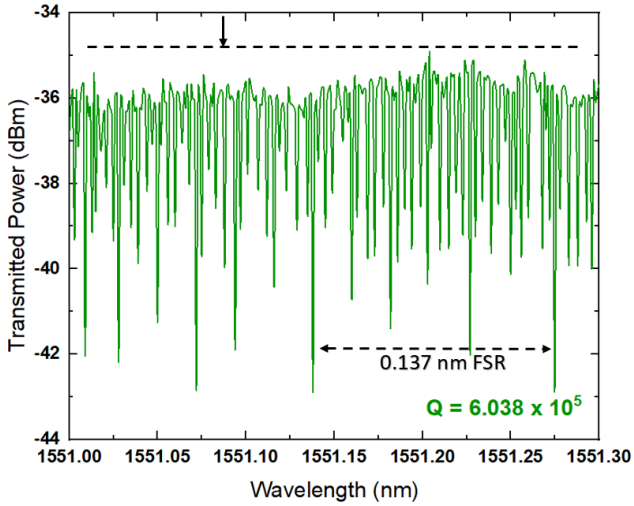

MBR-PVA-C

Fig. 3. The MBR-PVAs transmission spectral with resonant depths while coupled with microfiber 2µm diameter. The Q - factor changed due to the size of the resonator (color online)

The Q-factor is defined by estimation and Lorentziant fitting, where all sizes manage to have $>10^5$, which was acceptable as previous research [22, 41]. The estimation of the Q-facto is by $\lambda/\Delta\lambda$, where λ describe as the resonant frequency. The Lorentzian fitting is defined by Origin programming utilised. Fig. 3 showed the Q-factor of the MBR-PVA-C is the highest due to the size, which was largest among the rest, with $6.038x10^5$. The MBR-PVA-A and MBR-PVA-B managed to have $5.374x10^5$ and $5.791x10^{5,}$ respectively. The size of the MBR-PVA would determine the Q-factor and insertion loss. The free spectral range (FSR) depended on the MBR size, where the larger size of resonator causes the smallest value of FSR as showed in Fig. 3.

3. Performance of MBR-PVAs as Sodium Alginate Sensor

The MBR-PVAs was then used for sodium alginate concentration sensing, as shown in Fig. 4. The MBR-PVAs coupled with microfiber 2μm diameter allowed the WGMs spatially cross the resonator, which was then manipulated to be a sensing mechanism. One end of the microfiber is connected to the TLS for wavelength supplied, while another end is connected to an optical spectrum analyser for transmission spectral recorded. The experiment was conducted in a sealed chamber, which helps to remain the humidity and temperature level always at the same level. The observation began when the setup was supplied with a range of wavelengths as an input source. The sodium alginate is used from 1% to 6% concentration, with every output power from different liquid concentrations recorded. The same procedure was repeated by a three-time cycle, which may reduce random error during data collection. To increase the sensor's performance, it may remain 120 minutes long for the stability testing procedure. All the procedures applied for three sizes of MBR-PVAs. However, the input wavelength may be different due to the resonant depth's transmission spectral in Fig. 3. For example, the MBR-PVA-A used the input wavelength of 1551.065 nm, while the MBR-PVA-B and MBR-PVA-C may use 1551.063 nm and 1551.072 nm.

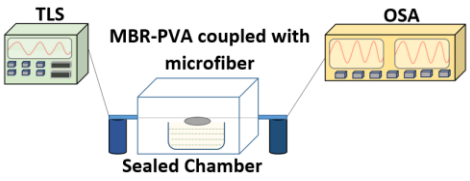

(a)

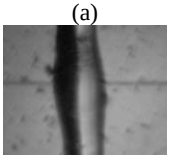

(b)

Fig. 4. The MBR-PVAs applied for sodium alginate concentration sensor (a) and the MBR couple with microfiber (b) (color online)

Every concentration of sodium alginate used may produce its wavelength shift. The shifting might differ for each coated resonator used. As mentioned in Fig. 5, the MBR-PVA-A wavelength shifted from 1551.064 nm to 1551.074 nm, MBR-PVA-B shifted from 1551.063 nm to 1551.076 MBR-PVA-C is from 1551.072 nm to 1551.087 nm. The shifting proves that the MBR-PVAs own their capability in molecule adsorption while used as a liquid sensor. It also showed that this coating MBR could be used as a liquid concentration sensor. The shifting interval showed by MBR-PVAs defined that the biggest size of coating resonator; MBR-PVA-C produce large wavelength shifting than others. It proved that the resonator's size influenced the MBR-PVA-C to have a large shifting on transmitted wavelength.

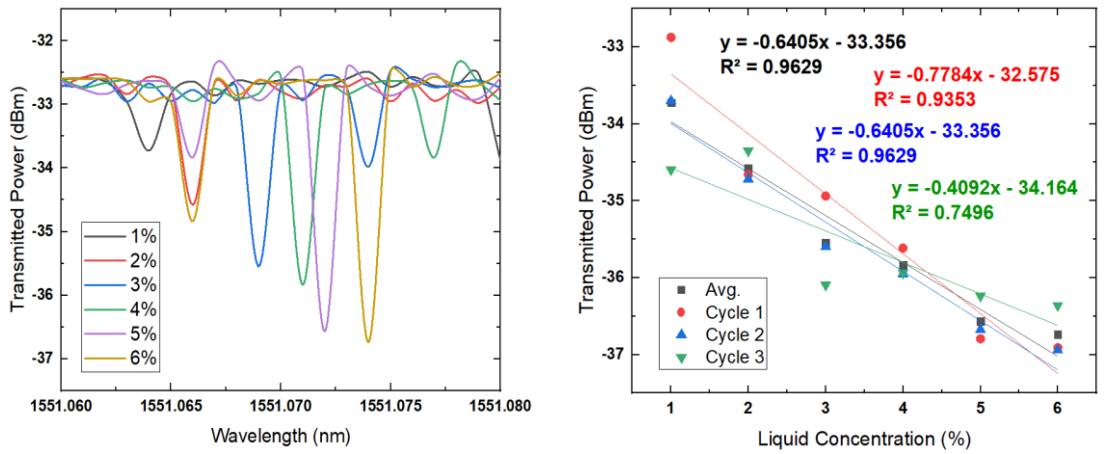

MBR-PVA-A

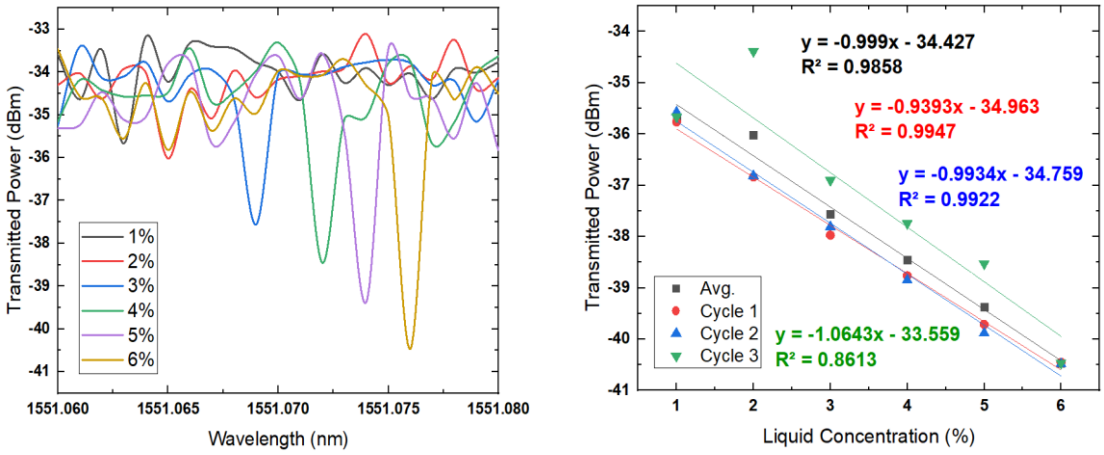

MBR-PVA-B

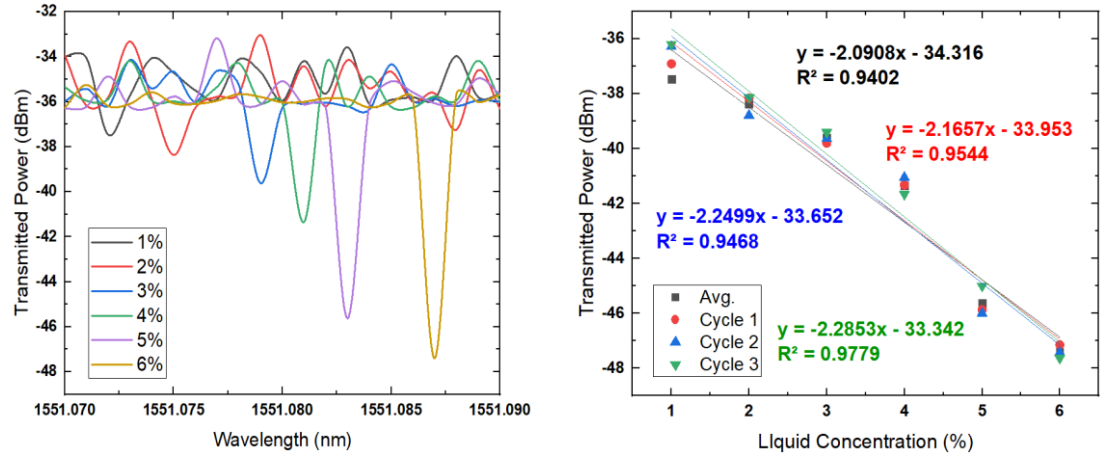

MBR-PVA-C

Fig. 5. The wavelength shift produced by different MBR-PVAs where the sensitivity, linearity and stability engaged with the shifting to determine the sensor performance (color online)

Fig. 5 showed the transmitted power decreased by increasing the value of the liquid concentration, respectively. The experiment repeated three cycles for each MBR-PVAs to reduce random error during data collections. Three cycles of repetition combined as average value define the sensitivity and linearity for each coating resonator. The linearity data of the MBR-PVAs showed some magnificent values that can have >90% for all conditions. The sensitivity value showed by the MBR-PVA-C is much higher with 2.0908 dB/%, where the MBR-PVA-B is only 0.999 dB/%, and the MBR-PVA-A is 0.6405 dB/%. By these results, the MBR-PVA-C showed the best performance as a sodium alginate concentration sensor. However, these sensitivity and linearity results were collected from transmitted power analysis compared with sensitivity and linearity collected from wavelength shift analysis. As shown in Fig. 6, the linearity may show tremendous results, where >90% for all conditions. The sensitivity of the MBR-PVA-C managed to have 2.9 pm/%, which was higher than MBR-PVA-A with 2.0 pm/% and MBR-PVA-B with only 2.7 pm/%. By these comparisons, the MBR-PVA-C, the largest coating resonator, showed the best performance as a sodium alginate sensor.

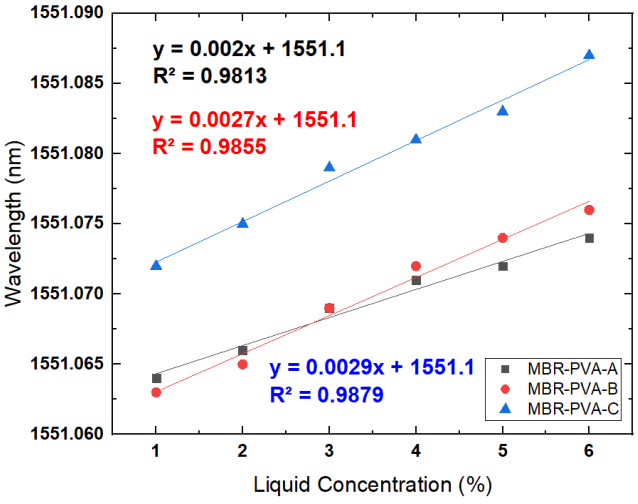

Fig. 6. The sensitivity and linearity performance by wavelength shifting analysis (color online)

The stability test was used to optimise the performance of MBR-PVAs as a sodium alginate concentration sensor. As shown in Fig. 7, the stability performance is then taken from 6% of liquid concentration. The coating resonator remained in this concentration for 120 minutes long. This may ensure that the MBR-PVAs may work for a long duration of time. Furthermore, the results showed that all MBR-PVA managed to remain in good condition with tremendous stability performance. This may confirm that the MBR-PVAs is suitable for use as a liquid concentration sensor.

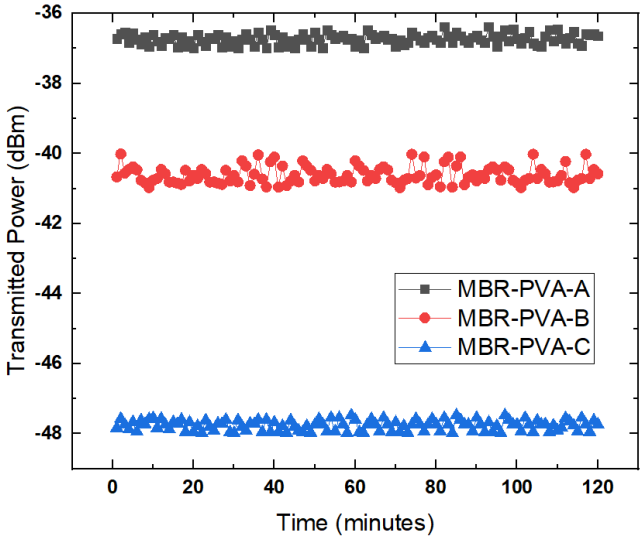

Fig. 7. The stability performance of MBR-PVAs as sodium alginate sensor (color online)

4. Conclusions

This experimental research paper investigated the performance of coated MBR as a sodium alginate concentration sensor. The MBR formed using the "soften-and-compress" technique, which then coated with PVA by the "drop-casting" method. Three coated MBR sizes named MBR-PVAs are then characterised using TLS and optical spectrum analyser. The MBR-PVAs produced transmitted spectral with different resonant depth values. The Q-factor is defined to have $>10^5$ for every coated MBR. The MBR-PVAs was then applied as the sodium alginate concentration sensor. The input wavelength might differ for each size of MBR-PVAs, based on the resonant depth from the transmitted spectral graph. Sensitivity, linearity, stability and repeatability are listed parameters used to indicate the best coated MBR performance as a sensor. The MBR-PVA-C, the biggest size among others, shows the best performance as a sodium alginate concentration sensor. This showed that the size might influence the coated MBR to perform well as a liquid sensor.

Acknowledgements

The work is funded by Research Development Grant Scheme RAGS/1/2014/SG04/UTEM/2. The authors would like to acknowledge Fakulti Teknologi Kejuruteraan Elektrik dan Elektronik Universiti Teknikal Malaysia Melaka, Fakulti Kejuruteraan Elektrik Universiti Teknikal Malaysia Melaka, Fakulti Kejuruteraan Elektronik dan Komputer Universiti Teknikal Malaysia Melaka and Faculty of Engineering, University of Malaya.

References

[1] H. H. M. Yusof, M. H. Jali, M. A. M. Johari, K. Dimyati, S. W. Harun, M. Khasanah, M. Yasin, IEEE Photonics Journal **11**(1), 1 (2019).

[2] H. H. M. Yusof, S. W. Harun, K. Dimyati, T. Bora, K. Sterckx, W. S. Mohammed, J. Dutta, IEEE Sensors Journal **19**(7), 2442 (2018).

[3] M. F. A. Rahman, M. F. M. Rusdi, A. R. Muhammad, A. A. Latiff, A. Ahmad, K. Dimyati, S. W. Harun, Journal of Physics: Conference Series, IOP Publishing **012008**(1), 1151 (2019).

[4] M. A. M. Johari, A. M. Azize, R. M. Said, N. A. Ngatiman, N. Zaine, MATEC Web of Conferences, EDP Sciences **01108**, 97 (2017).

[5] M. Yasin, Z. Jusoh, H. A. Rahman, M. D. Ashadi, S. W. Harun and H. Ahmad, J. Optoelectron. Adv. M. **13**(10), 1199 (2011).

[6] M. H. Jali, H. R. A. Rahim, M. A. M. Johari, S. S. Hamid, H. H. M. Yusof, S. Thokchom, K. Dimyati, S. W. Harun, Journal of Physics: Conference Series, IOP Publishing **012006**(1), 1151 (2019).

[7] M. A. M. Johari, M. I. M. A. Khudus, M. H. B. Jali, A. Al Noman, S. W. Harun, Optik **185**, 558 (2019).

[8] M. A. M. Johari, M. A. Khudus, A. Al Noman, M. H. Jali, H. H. M. Yusof, S. W. Harun, M. Yasin, Journal of Physics: Conference Series, IOP Publishing **012021**(1), Vol. 1151 (2019).

[9] X. Tian, K. Powell, L. Li, S. X. Chew, X. Yi, L. Nguyen, R. A. Minasian, Journal of Lightwave Technology **38**(19), 5440 (2020).

[10] N. Pala, M. Shur, Micro-and Nanotechnology Sensors, Systems, and Applications XI, International Society for Optics and Photonics **109822Y**, 10982 (2019).

[11] M. Zhang, B. Buscaino, C. Wang, A. Shams-Ansari, C. Reimer, R. Zhu, J. M. Kahn, M. Lončar, Nature **568**(7752), 373 (2019).

[12] M. Esmann, F. R. Lamberti, A. Harouri, L. Lanco, I. S. A. B. E. L. L. E. Sagnes, I. Favero, G. Aubin, C. Gomez-Carbonell, A. Lemaitre, O. Krebs, P. Senellart, Optica **6**(7), 854 (2019).

[13] A. Daraei, M. E. Daraei, Applied Physics A **123**(4), 216 (2017).

[14] A. Pauls, I. Lekavicius, H. Wang, Frontiers in Optics, Optical Society of America JW6A-2 (2020).

[15] Y. L. Chen, W. L. Jin, Y. F. Xiao, X. Zhang, Physical Review Applied **6**(4), 044021 (2016).

[16] L. Wu, H. Wang, Q. Yang, Q. X. Ji, B. Shen, C. Bao, M. Gao, K. Vahala, Optics Letters **45**(18), 5129 (2020).

[17] M. A. M. Johari, M. I. M. A. Khudus, M. H. B. Jali, A. Al Noman, S. W. Harun, Sensors and Actuators A: Physical **284**, 286 (2018).

[18] M. H. Jali, H. R. A. Rahim, S. S. Hamid, M. A. M. Johari, H. H. M. Yusof, S. Thokchom, S. W. Harun, M. Khasanah, M. Yasin, Optik **196**, 163174 (2019).

[19] P. Bianucci, Sensors **16**(11), 1841 (2016).

[20] G. Nemcova, R. Kashyap, Journal of Lightwave Technology **25**(8), 2244 (2007).

[21] M. N. M. Nasir, G. S. Murugan, M. N. Zervas, IEEE Photonics Conference (IPC) 759-760 (2016).

[22] A. Chiasera, Y. Dumeige, P. Feron, M. Ferrari, Y. Jestin, G. Nunzi Conti, S. Pelli, S. Soria, G. C. Righini, Laser & Photonics Reviews **4**(3), 457 (2010).

[23] A. B. Matsko, A. A. Savchenkov, D. Strekalov, V. S. Ilchenko, L. Maleki, IPN Progress Report **42**(162), 1 (2005).

[24] P. Berini, Advances in Optics and Photonics **1**(3), 484 (2009).

[25] M. A. M. Johari, M. I. M. A. Khudus, M. H. B. Jali, M. S. Maslinda, U. U. M. Ali, S. W. Harun, A. H. Zaidan, R. Apsari, M. Yasin, Sensing and Bio-Sensing Research **25**, 100292 (2019).

[26] M. A. M. Johari, A. H. Rosol, N. A. Baharuddin, M. I. M. A. Khudus, M. H. Jali, M. S. Maslinda, S. S. Jaapar, S. W. Harun, IOP Conference Series: Materials Science and Engineering, IOP Publishing **012075**(1), 854 (2020).

[27] M. A. M. Johari, M. P. Pour, A. Al Noman, M. I. M. A. Khudus, M. H. Jali, M. S. Maslinda, U. U. M. Ali, S. W. Harun, Microwave and Optical Technology Letters **62**(3), 993 (2020).

[28] M. A. M. Johari, M. I. M. A. Khudus, M. H. Jali, A. N. Abdullah, S. W. Harun, Journal of Physics: Conference Series, IOP Publishing Ltd. **1-8**, 1371 (2019).

[29] M. A. M. Johari, A. Al Noman, M. I. M. A. Khudus, M. H. Jali, H. H. M. Yusof, S. W. Harun, M. Yasin, Optik **173**, 180 (2018).

[30] S. Abbasiliasi, T. J. Shun, T. A. T. Ibrahim, N. Ismail, A. B. Ariff, N. K. Mokhtar, S. Mustafa, RSC Advances **9**(28), 16147 (2019).

[31] S. Fu, A. Thacker, D. M. Sperger, R. L. Boni, I. S. Buckner, S. Velankar, E. J. Munson, L. H. Block, Aaps Pharmscitech **12**(2), 453 (2011).

[32] P. Hu, X. Dong, W. C. Wong, L. H. Chen, K. Ni, C. C. Chan, Applied Optics **54**(10), 2647 (2015).

[33] P. Hu, X. Dong, W. C. Wong, L. H. Chen, K. Ni, C. C. Chan, Journal of Biomedical Optics **16**(7), 077001 (2011).

[34] J. M. Ward, D. G. O'Shea, B. J. Shortt, M. J. Morrissey, K. Deasy, S. G. Nic Chormaic, Review of Scientific Instruments **77**(8), 083105 (2006).

[35] G. S. Murugan, M. N. Petrovich, Y. Jung, J. S. Wilkinson, M. N. Zervas, Optics Express **19**(21), 20773 (2011).

[36] N. M. Isa, N. Irawati, H. A. Rahman, M. H. M. Yusoff, S. W. Harun, IEEE Sensors Journal **18**(7), 2801 (2018).

[37] N. M. Isa, N. Irawati, S. W. Harun, F. Ahmad, H. A. Rahman, M. H. M. Yusoff, Sensors and Actuators A: Physical **272**, 274 (2018).

[38] M. N. M. Nasir, G. S. Murugan, M. N. Zervas, Photonics Conference (IPC), IEEE 759-760 (2016).

[39] M. Cai, O. Painter, K. J. Vahala, Physical Review Letters **85**(1), 74 (2000).

[40] M. N. M. Nasir, G. S. Murugan, M. N. Zervas, J. Opt. Soc. Am. B **33**(9), 1963 (2016).

[41] M. A. M. Johari, M. I. M. A. Khudus, M. H. B. Jali, A. Al Noman, S. W. Harun, Sensors and Actuators A: Physical **284**, 286 (2018).

*Corresponding author: aminah@utem.edu.my